International Journal of Adhesion & Adhesives 123 (2023) 103342

Contents lists available at ScienceDirect

International Journal of Adhesion and Adhesives

journal homepage: www.elsevier.com/locate/ijadhadh

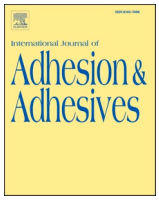

Structural and adhesion properties of waterborne polyurethane adhesives containing nanosilica dispersion obtained with different physical mixing procedures

M. Echarri-Giacchi, J.M. Martín-Martínez *

Adhesion and Adhesives Laboratory, University of Alicante, 03080, Alicante, Spain

ARTICLE INFO

Keywords:
Waterborne polyurethane
Nanosilica dispersion
Physical mixing
Phase separation
Thermal properties
Adhesion

ABSTRACT

Nanosilica dispersion was added to waterborne polyurethane dispersion by using three different physical mixing procedures differing in the flow regime (tangential, laminar, radial) and the stirring rate (300–2400 rpm). The influence of the physical mixing procedure on the structural, thermal, rheological, mechanical, surface and adhesion properties of the polyurethanes (PUs) containing 1 wt% nanosilica was evaluated. The nanosilica in the dispersion was functionalized with acrylic moieties and showed high surface tension and negative Z potential values. The PU + nanosilica blend made with higher shear rate and laminar flow regime showed high homogeneous dispersion of the nanosilica particles and greater extent of intercalation between the soft segments of the polyurethane, this led to higher thermal stability. Unexpectedly, the better dispersion of the nanosilica in the PU matrix decreased the wettability of the PU + nanosilica materials due to the migration of acrylic moieties from the nanosilica particles to the surface. As a consequence, a decrease of the final T-peel strength was found. However, the single lap-shear strength did not change by adding nanosilica because of the scarce improvement of the mechanical properties in the PU + nanosilica materials.

1. Introduction

Waterborne polyurethane dispersions (PUDs) are multiphasic systems made of spherical nanoparticles dispersed in water. PUDs are synthesized by reacting a diisocyanate, a polyol, an internal emulsifier and a chain extender, the internal emulsifier anchors covalently pendant ionic or non-ionic moieties in the linear polyurethane chain which are oriented outside of the particles in the presence of water. There are several methods of synthesis of the PUDs, the prepolymer and the acetone methods are the most commonly used [1].

Waterborne polyurethane adhesives are generally made by mixing PUD with a thickener and a wetting agent, and their properties are mainly determined by the ones of the PUD. Because of health and environment concerns, these adhesives are currently substituting the solvent born polyurethane adhesives in several applications in the furniture, automotive, textile and footwear industries. Although effective, the waterborne polyurethane adhesives have limited water resistance, relative low thermal resistance and insufficient mechanical properties [2]. For improving these properties, several strategies have been proposed including the addition of cross-linkers [3] and fillers [4], among other. Recently, the addition of small amounts (0.01–0.10 wt%) of graphene oxide filler has been proposed successfully for improving the mechanical and adhesion properties of the waterborne polyurethane dispersions [5], but the graphene oxide is expensive and difficult to disperse in water-based systems.

Fumed silica fillers have been commonly added for improving the rheological, mechanical and adhesion properties of the solvent born polyurethane adhesives [6]. The improved properties of these silica-polyurethane adhesives have been ascribed to the interactions by hydrogen bonds between the silanol groups on the silica surface and the urethane/urea groups of the polyurethane chains [7]. However, the addition of fumed silicas to PUDs is not effective due to the formation of silica agglomerates and the phase separation of the polyurethane micelles in the dispersion [8]. Therefore, different procedures have been proposed for incorporating silica fillers in PUDs, including the sol-gel method [9–17], the in-situ polymerization of the silica precursor [2,18–23], the use of silica as chain extender during the synthesis of the PUD [24–28], the click-chemistry of the silica precursor [29,30], and the physical mixing of the PUD and nanosilica dispersion [31–37], the sol-gel method is the most commonly used. Although the incorporation

* Corresponding author.
E-mail address: jm.martin@ua.es (J.M. Martín-Martínez).

https://doi.org/10.1016/j.ijadhadh.2023.103342
Received 11 September 2022; Received in revised form 21 January 2023; Accepted 11 February 2023
Available online 18 February 2023
0143-7496/© 2023 The Authors. Published by Elsevier Ltd. This is an open access article under the CC BY-NC-ND license (http://creativecommons.org/licenses/by-nc-nd/4.0/).

of silica precursors during the polyurethane synthesis is efficient for producing hybrid silica-waterborne polyurethane dispersions, their stabilities and adhesion properties are limited, the physical mixing of the PUD and nanosilica dispersions is more simple, this procedure has been selected in this study.

There are some previous studies comparing the influence of the procedure of adding silica on the properties of the PUDs. Heck et al. [14] compared the properties of silica-PUD dispersions made by in-situ silica formation from tetraethyl *ortho*-silicate – TEOS – precursor during the synthesis of the PUD with the one obtained by physical mixing of the PUD and a colloidal nanosilica of 9 nm primary particle size. Whereas the PUD synthesized with TEOS showed some silica agglomerates, the physical mixing caused poor interactions between the substrate and the PUD + silica material, and decreased adhesion was obtained. In a later study [35], the performance of silica-PUD composites obtained with TEOS precursor during the PUD synthesis and the physical mixing of PUD and silica dispersion was compared, the procedure of adding the silica and the silica nature determined differently the properties. Thus, the mechanical properties of the PUD were improved by physical mixing, but the adhesion was better by in-situ formation of the silica; furthermore, the study concluded that the addition of silica increased the degree of phase separation in the polyurethane. In the last years, PUDs containing spherical nanosilica particles of less than 100 nm diameter have been synthesized by using 3-aminopropyl triethoxisilane (APTES) as main precursor, their adhesion properties were not studied [38,39].

Some previous studies have explored the properties of PUDs containing nanosilica prepared by physical mixing. Yan et al. [31] added up to 50 wt% colloidal nanosilica of 25 nm diameter to PUD by mechanical stirring, and, although some silica agglomerates were obtained, the thermal and mechanical properties were improved. Chiacchiarelli et al. [40] have synthesized silica-waterborne polyurethanes containing 1 wt % silica by using different physical mixing procedures (ultrasonic bath, high shear dissolver – 15,000 rpm for 20 min) and nanosilicas (hydrophilic nanosilica, calcined silica, hydrophobic silica), they concluded that the nature of the silica determined the extent of the dispersion of the silica and the ultrasonic bath provided lower degree of silica agglomeration. Serkis et al. [33] have synthesized silica-waterborne polyurethanes containing 5, 32 y 50 wt% of two anionic colloidal silicas of different primary particle sizes by physical mixing, they concluded that the addition of the silica with lower particle size (12 nm) provided better properties. Recently, Boonsong and Khaokong [37] have obtained silica-waterborne polyurethanes containing up to 5 wt% silica by mechanical stirring, the source of silica was rice husk modified with polydiallildimethylammonium salt. They found improved thermal properties by adding less than 1.5 wt% rice husk, but the mechanical properties of the PUD were deteriorated due to the sedimentation of the rice husk particles.

There are few studies on the adhesion of PUDs containing silicas. Cackić and col [32]. synthesized silica-polyurethane dispersions by adding 0.5–1 wt% hydrophilic nanosilica dispersion under vigorous stirring (1000–1300 rpm), the adhesion of the coatings evaluated by cross-cut test was improved. Later, the same authors [15] synthesized hybrid silica-polyurethane dispersions with 0.5–2 wt% APTES by using the sol-gel method, the adhesion of the silica-PUD coatings evaluated by cross-cut test was not improved due to poor silica-polyurethane interactions. Jia-Hu et al. [2] also synthesized hybrid silica-polyurethane dispersions containing 1–3 wt% silica by in-situ polymerization, the adhesion evaluated by T-peel and single lap-shear tests was improved by adding less than 2 wt% silica. The improved adhesion was ascribed to the creation of hydrogen bonds between the silica and the urethane groups.

The previous studies on the silica-waterborne polyurethane materials have shown that the main limitation is the adequate dispersion of the silica, the procedure of adding/dispersing the silica is critical. Furthermore, the previous literature related to the influence of adding silica on the mechanical and adhesion properties of the PUDs are not conclusive. Therefore, the main objective of this study is the addition of nanosilica dispersion to PUD by using different physical mixing procedures and establish their influence on the structural, thermal, rheological, mechanical and adhesion properties of the silica-PUD dispersions. Furthermore, a small amount of nanosilica was selected (a nanosilica dispersion of 12 nm primary size containing 1 wt% nanosilica) for being added to PUD by using three different physical mixing procedures that differ in the stirring rate and the rheological flow regime.

2. Experimental

2.1. Materials

Anionic waterborne polyurethane dispersion Dispercoll® U56 (Covestro, Leverkusen, Germany) and colloidal nanosilica dispersion LUDOX® AM (Grace, Columbia, USA) with nominal primary particle size of 12 nm were used.

2.2. Physical mixing of the nanosilica and waterborne polyurethane dispersions

Nanosilica dispersion containing 1 wt% nanosilica was added to the waterborne polyurethane dispersion by using three different physical mixing procedures that differ in the stirring rate and the rheological flow regime.

- Anchor stirrer and low stirring rate. 182.5 mL PUD was added into 1 L baker and stirred with Heidolph RZR 2020 stirrer (Heidolph, Schwabach, Germany) at 200 rpm for 15 min - Fig. 1. Then, 2.9 mL nanosilica dispersion (equivalent to 1 wt% nanosilica) was added drop by drop. Tangential flow regime was produced and the angular rate was 0.84 m/s. The nomenclature of the waterborne polyurethane dispersion consists in the capital letters "PUD" followed by "+" and the letters "SiH". The nomenclature of the solid waterborne

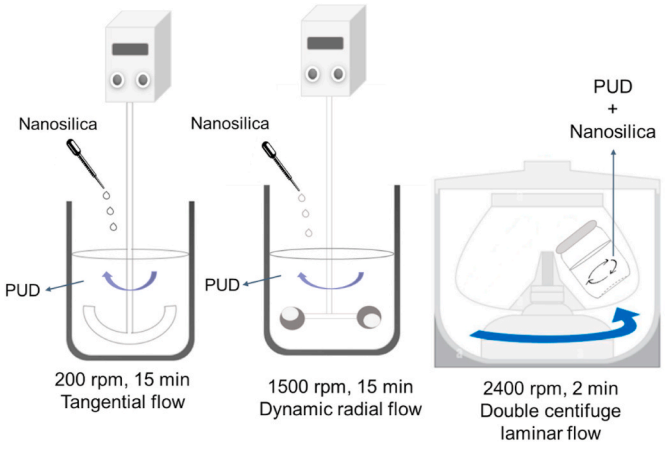

Fig. 1. Scheme of the physical mixing procedures of the PUD and the nanosilica dispersion. (Left) Anchor stirrer; (Centre) ViscoJet® stirrer; (Right) Double centrifuge SpeedMixer® stirrer.

- Double centrifugal SpeedMixer® and high stirring rate. 182.5 mL PUD and 2.9 mL nanosilica dispersion were added into propylene flask which was closed with propylene cover lid. The mixture was placed in a SpeedMixer® DAC 150.1 FVZ equipment (Hauschild Engineering, Hamm, Germany) and stirred at 2400 rpm for 2 min - Fig. 1. Laminar flow regime was produced. The nomenclature of the waterborne polyurethane dispersion consists in the capital letters "PUD" followed by "+" and the letters "SiSM". The nomenclature of the solid waterborne polyurethane containing nanosilica was similar, but the capital letters "PUD" were changed by "PU".

polyurethane containing nanosilica was similar, but the capital letters "PUD" were changed by "PU".

- ViscoJet® stirrer and high stirring rate. 182.5 mL PUD was added into 1 L baker and stirred with Heidolph RZR 2020 stirrer (Heidolph, Schwabach, Germany) at 1500 rpm for 15 min - Fig. 1. Then, 2.9 mL nanosilica dispersion (equivalent to 1 wt% nanosilica) was added drop by drop. Dynamic radial flow regime was produced and the angular rate was 1.9 m/s. The nomenclature of the waterborne polyurethane dispersion consists in the capital letters "PUD" followed by "+" and the letters "Si2H". The nomenclature of the solid waterborne polyurethane containing nanosilica was similar, but the capital letters "PUD" were changed by "PU".

Solid polyurethane (PU) and PU + nanosilica films were obtained by placing 20 mL dispersion in square Teflon mould of dimensions 120 mm × 200 mm x 1 mm. The water was removed at room temperature for 1 week.

2.3. Experimental techniques

2.3.1. Characterization of the nanosilica powder

Nanosilica powder was obtained by placing 10 mL nanosilica dispersion in open Teflon mould allowing the water evaporation at room temperature for 3 days. The solid nanosilica was crushed in agate mortar and sieved for obtaining a fine and homogeneous powder.

The nanosilica powder was characterized by X-ray fluorescence, elemental analysis, infra-red (IR) spectroscopy, X-ray photoelectron spectroscopy and transmission electron microscopy.

X-ray-fluorescence. The elemental analysis of the nanosilica powder was carried out by X-ray fluorescence in a Philips MagiX pro PW2400 equipment (Eindhoven, The Netherlands) provided with Rhodium tube and Berilium window.

Elemental analysis. The existence of carbon, hydrogen, nitrogen and oxygen in the nanosilica powder was determined in a Micro TruSpec LECO analyzer (LECO Instrumentos S.L., Tres Cantos, Madrid) under helium flow. Infra-red and thermal conductivity detectors were used.

Attenuated total reflectance Fourier transform infrared (ATR-IR) spectroscopy. Nanosilica tablet of dimensions 13 mm × 15 mm was obtained by pressing 0.5 g powder in a Specac 13 mm Pellet Die press (Orpington, UK) at 0.4 MPa for 20 s. The ATR-IR spectrum of the nanosilica tablet was obtained in an Alpha FT-IR spectrometer (Bruker Optik GmbH, Ettlinger, Germany) by using a germanium prism. 64 scans with a resolution of 4 cm^{-1} were recorded and averaged, an incident angle of the IR beam of 45° was used.

X-ray photoelectron spectroscopy (XPS). The chemical composition of the nanosilica powder surface was determined by XPS in a K-Alpha Thermo-Scientific spectrometer (Waltham, Massachusetts, USA), an Al-Kα X-ray source (1486.6 eV) was used. XPS survey spectrum was collected in the range of binding energies between 0 and 1200 eV, using a spot size of 300 μm and pass energy of 150 eV. High-resolution spectra of all elements were obtained over a 20 eV range.

Transmission electron microscopy (TEM). The morphology of the nanosilica powder was determined in a Jeol JEM-1400 Plus instrument (Jeol, Tokyo, Japan) by using an acceleration voltage of 120 kV. Prior to analysis, the nanosilica dispersion was diluted in 2-propanol and the solution was placed in ultrasonic bath for 60 s. One drop of solution was placed on a carbon grid for analysis, allowing the evaporation of the solvent at room temperature for 2 days before analysis.

2.3.2. Characterization of the nanosilica dispersion and the waterborne polyurethane dispersions (PUDs) without and with nanosilica

Solids content. The solids contents of the nanosilica dispersion and the PUDs without and with nanosilica were determined in a DBS 60–3 thermo balance (Kern & Sohn GmbH, Balingen, Germany). About 0.5 g dispersion was heated at 105 °C for 15 min followed by heating at 120 °C until a constant mass was obtained. For each sample, three replicates were measured and averaged.

pH *measurement*. About 25 cm^3 of the nanosilica dispersion and the PUDs without and with nanosilica were placed in a beaker and the pH value was measured at 21 °C in a pH-meter PC-501 (XS Instruments, Carpi, Italy) equipped with XC-PC510 electrode. For each sample, three replicates were measured and averaged.

Brookfield viscosity. The viscosities of the nanosilica dispersion and the PUDs without and with nanosilica were measured at 22 °C in a Brookfield RD DV-I Prime (Brookfield Engineering Laboratories Inc., Stoughton, DE, USA) according to ASTM D3236-88 standard. 150 mL dispersion were placed in 250 mL beaker and, after introducing the spindle, the shear rate was increased until the viscometer went out scale. S-61 spindle was used for the nanosilica dispersion and S-62 spindle was used for the PUDs without and with nanosilica. For each sample, three replicates were measured and averaged.

Surface tension. The surface tensions of the nanosilica dispersion and the PUDs without and with nanosilica were measured at 22 °C in a Phywe equipment (Göttingen, Germany) by using a metallic ring of 19.5 mm diameter, the DuNouy ring method was used. For each sample, three replicates were measured and averaged.

Particle size distribution. The particle size distributions of the nanosilica in the dispersion and in the PUDs without and with nanosilica were determined by dynamic light scattering in a Microtrac Sync equipment (Verder Scientific group, Haan, Duesseldorf, Germany). Blue (405 nm) and red (708 nm) lasers were used. Before analysis, the PUDs were diluted in deionized water.

Z potential. The Z potentials of the nanosilica dispersion and the PUDs without and with nanosilica were measured in a Nanotrac Flex (Microtrac Mrb, Verder Scientific group, Dusseldorf, Germany) combined with Stabino equipment (Colloid Metrix, GmbH, Meerbusch, Germany). Blue (405 nm) and red (708 nm) lasers were used. Before analysis, the PUDs were diluted in deionized water.

2.3.3. Characterization of the solid waterborne polyurethane without (PU) and with nanosilica (PU + nanosilica) materials

Attenuated total reflectance Fourier transform infrared (ATR-IR) spectroscopy. The ATR-IR spectra of the PUs without and with nanosilica were obtained in an Alpha FT-IR spectrometer (Bruker Optik GmbH, Ettlinger, Germany) by using a germanium prism. 64 scans with a resolution of 4 cm^{-1} were recorded and averaged, an incident angle of the IR beam of 45° was used. Two replicates for each sample were obtained.

Differential scanning calorimetry (DSC). The DSC curves of the PUs without and with nanosilica were obtained in a TA DSC Q100 V6.2. Equipment (TA Instruments, New Castle, DE, USA). Aluminium pans containing 10–15 mg sample were heated from −80 to 200 °C under nitrogen atmosphere (flow rate: 50 mL/min), the heating rate was 10 °C/min. Then a cooling run from 200 °C to −80 °C was carried out by using a cooling rate of 10 °C/min, and finally a second DSC heating run from −80 to 250 °C was carried out by using a heating rate of 10 °C/min. Two replicates for each sample were obtained.

Thermal gravimetric analysis (TGA). The structure and the thermal properties of the PUs without and with nanosilica were assessed in a TGA Q500 equipment (TA Instruments, New Castle, DE, USA). 10–15 mg PU were placed in platinum crucible and heated under nitrogen (flow rate: 100 mL/min) from room temperature up to 600 °C, by using a heating rate of 10 °C/min. Two replicates for each sample were obtained.

Plate-plate rheology. The rheological and viscoelastic properties of the PUs without and with nanosilica were measured in a DHR-2 rheometer (TA Instruments, New Castle, DE, USA) by temperature sweeps experiments, parallel plates (upper plate diameter = 25 mm) geometry was used. The gap was 400 μm. The solid sample was placed on the bottom plate heated at 140 °C and allowed to melt for setting the gap. The measurements were carried out by decreasing the temperature from 140 to 10 °C in Peltier system, a cooling rate of 5 °C/min and a frequency of 1 Hz were used. The rheological experiments were performed in the

region of linear viscoelasticity. Two replicates for each sample were obtained.

Stress-strain tests. Thin PU films without and with nanosilica for stress-strain tests were prepared by placing 10 g dispersion on glass coated Teflon® substrate of dimensions 12 mm × 24 mm. Three pieces of double side tape (3 M, St Paul, Minnesota, USA) were placed over the sides of the mould for adjusting a thickness of 200 μm; once the dispersion was spread over the mould, the water was left evaporate at room temperature for four days, the thicknesses of the test samples were about 60 μm. The mechanical properties of the PUs without and with nanosilica were assessed by stress-strain tests according to ISO 37 standard. Dog-bone test specimens were cut and the stress-strain tests were carried out in a Zwick/Roell Z005 universal testing machine (San Cugat del Vallés, Spain) provided with mechanical extensometer, a pulling rate of 100 mm/min was used. Five replicates were measured and averaged.

Water contact angle measurements. The contact angle measurements were carried out at 21 °C by using bi-distilled and deionized water. The water contact angles were measured on the surfaces of the PU films in an ILMS goniometer (GBX Instruments, Bourg de Pèage, France). At least five water droplets of 4 μL were placed on different locations of each PU film surface, and the water contact angles were averaged.

Transmission electron microscopy (TEM). The dispersion of the nanosilica in the PU + nanosilica materials was determined in a Jeol JEM-1400 Plus instrument (Jeol, Tokyo, Japan) by using an acceleration voltage of 120 kV. Prior to analysis, one drop of PU + nanosilica dispersion was placed on a carbon grid allowing the evaporation of the water at room temperature for 2 days before measurement.

2.3.4. Adhesion measurement

Single lap-shear test of stainless steel/PUD/stainless steel joints. The adhesion of the PUDs without and with nanosilica was determined by single lap-shear tests of stainless steel/PUD/stainless steel joints. Stainless steel 304 specimens with dimensions of 30 mm × 150 mm x 1 mm were used and they were mechanically abraded with green fibre 3 M scouring pad (Scotch Brite®) followed by wiping with isopropanol, leaving it evaporates at room temperature for 5 min. Then, 0.05 g dispersion were placed with a Pasteur pipette on 20 mm × 30 mm side surface on one of the stainless steel specimens and, then, the other stainless steel specimen was placed on top, applying a pressure of 0.13 MPa at room temperature. After 72 h, the single lap-shear tests were carried out in a Zwick/Roell Z005 universal testing machine (San Cugat del Vallés, Spain), a crosshead speed of 10 mm/min was used. At least five replicates for each adhesive joint were determined and averaged. The loci of failure of the joints were assessed by visual inspection.

T-peel tests of plasticized poly(vinyl chloride) (PVC)/PUD/plasticized PVC joints. The adhesive strengths of the joints made with PUDs without and with nanosilica were obtained from T-peel tests of plasticized PVC/PUD/plasticized PVC joints. The plasticized PVC test samples had dimensions of 30 mm × 150 mm × 4 mm and they were methyl ethyl ketone wiped for plasticizer removal, allowing the solvent to evaporate for 30 min under open air. Then, 3 mL PUD was applied by brush to each PVC strip and, after water evaporation at 25 °C for 1 h, the adhesive film was melted suddenly at 85 °C for 10 s under infrared radiation (reactivation process). The PVC strips were immediately placed in contact and a pressure of 0.4 MPa was applied for 10 s to achieve a suitable joint. The T-peel strength was measured 15 min (immediate adhesion) and 72 h (final adhesion) after joint formation in a Zwick/Roell Z005 universal testing machine (San Cugat del Vallés, Spain), a crosshead speed of 100 mm/min was used. Five replicates were measured and averaged. The loci of failure of the joints were assessed by visual inspection.

3. Results and discussion

3.1. Characterization of the nanosilica dispersion and powder

The nanosilica dispersion contains 28.9 wt% nanosilica and has a basic pH (9.2 ± 0.1). The Z-potential value is −87 mV denoting a negative surface charge and high stability. On the other hand, the nanosilica dispersion shows a Newtonian rheological behavior, the Brookfield viscosity is quite low (11 ± 2 mPa s) and the surface tension is somewhat high (62.9 mN/m).

The particle size distribution of the nanosilica dispersion is multimodal (Fig. 2) and consists in 1% nanosilica particles of 12 nm, 11% nanosilica particles of 140 nm and 88% nanosilica particles of 768 nm. Therefore, the most nanosilica particles are agglomerated. In fact, the TEM micrographs of the nanosilica dispersion show a few individual spherical nanosilica particles (they are marked with red arrows in Fig. 3), the most particles are clustered forming agglomerates of about 150 nm. Because the different preparation of the samples used in the two experimental techniques for determining the distribution of the nanosilica particles, different quantitative results are obtained. However, both methods show that the most nanosilica particles are clustered.

The nanosilica dispersions are generally produced by adding surfactants [41] or by functionalization of nanosilica particles with acrylic moieties [42], among other. Therefore, the agglomeration of the nanosilica particles in the dispersion should be ascribed to the interactions between the negative polar moieties on the surface rather to the interactions between the superficial silanol groups.

The nanosilica powder obtained by drying the dispersion was characterized by ATR-IR spectroscopy, XPS, elemental analysis, and X-ray fluorescence.

The elemental analysis of the nanosilica powder shows the existence of 0.06 at.% carbon and 0.99 at.% hydrogen, indicating the existence of organic carbon moieties that should derive from the functionalization moieties. Furthermore, the X-ray fluorescesce of the nanosilica powder shows the existence of 45.80 at.% silicon, 52.90 at.% oxygen, 0.86 at.% sodium and impurities of aluminium and sulfur (0.37 at.% aluminium and 0.07 at.% sulfur). The oxygen content in the nanosilica powder is lower than expected from the stoichiometry of SiO_2 because double amounts of oxygen atoms than silicon atoms should be obtained, this indicates the existence of moieties containing carbon, oxygen and hydrogen in the nanosilica powder.

The ATR-IR spectrum of the nanosilica powder (Fig. 4) shows the typical Si–O bending band at 798 cm^{-1} and the asymmetric Si–O–Si stretching bands at 1106 and 962 cm^{-1} of silica. Furthermore, a band at 3370 cm^{-1} due to Si–OH stretching and adsorbed water and another at 1621 cm^{-1} due to C═C stretching [43] can be distinguished, the existence of these bands confirms the presence of functionalized nanosilica particles with C═C containing moieties, likely acrylic species.

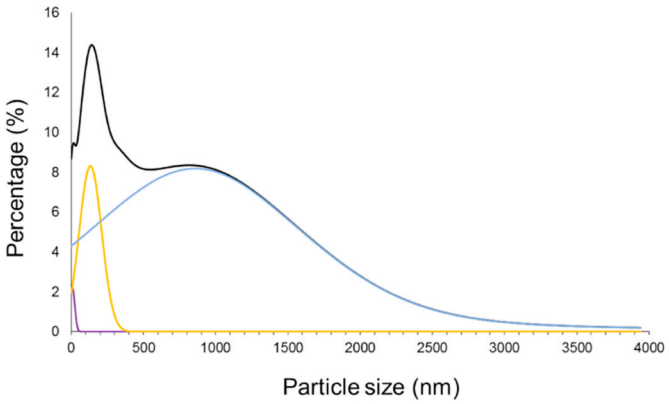

Fig. 2. Particle size distribution of the nanosilica dispersion.

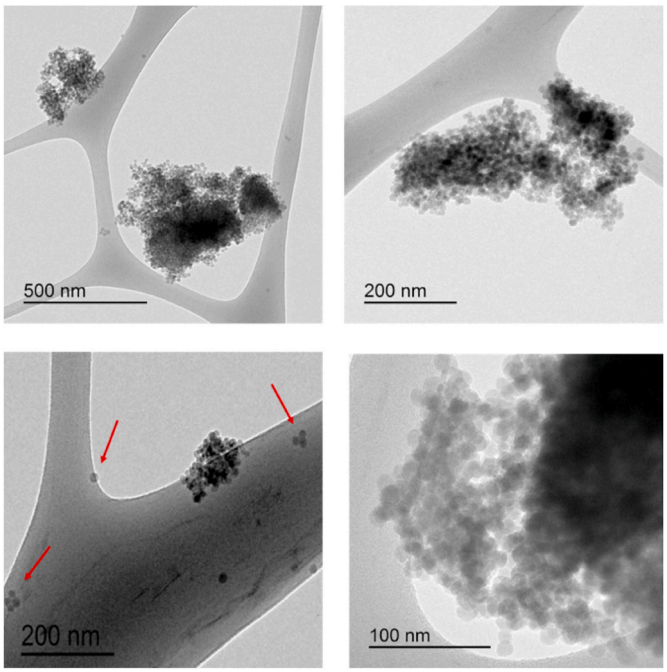

Fig. 3. TEM micrographs of the nanosilica particles. The carbon grid can be distinguished in the TEM micrographs.

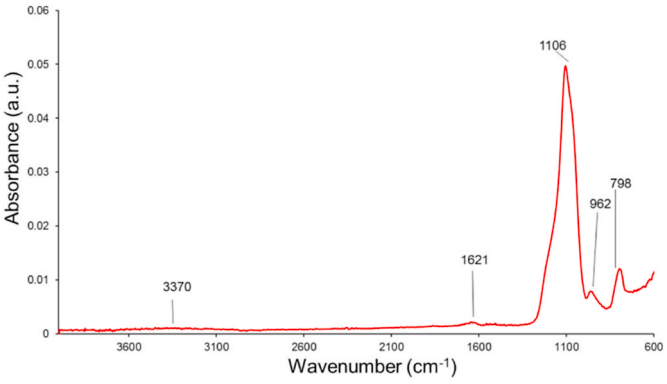

Fig. 4. ATR-IR spectrum of the nanosilica powder.

The chemical composition of the nanosilica powder surface was analyzed by XPS. The nanosilica powder surface contains 56.3 at.% oxygen, 40.2 at.% silicon, 2.5 at.% carbon, 0.9 at.% sodium and traces of chlorine. Therefore, the nanosilica powder surface is functionalized with carbon and oxygen containing species. The nature of the chemical groups on the nanosilica powder surface was assessed from the high resolution XPS spectra of silicon, oxygen and carbon (Fig. 5). The curve fitting of Si2p high resolution XPS spectrum shows two contributions due to Si–O–Si (60 at.%) at binding energy of 103.0 eV and Si–OH (40 at.%) at binding energy of 103.8 eV on the nanosilica powder surface [44]. On the other hand, the curve fitting of O1s high resolution XPS spectrum shows two contributions due to Si–O–Si and C═O (95 at.%) at binding energy of 532.6 eV and C–O (5 at.%) at binding energy of 533.9 eV on the nanosilica powder surface [45], they correspond to acrylic moieties. The existence of acrylic moieties on the nanosilica powder surface is also confirmed by the curve fitting of C1s high resolution XPS spectrum that shows three contributions due to C–C and Si–C (80 at.%) at binding energy of 285.0 eV, C–O (4 at.%) at binding energy of 287.0 eV, and –O═C–OH (16 at.%) at binding energy of 289.0 eV [42].

In summary, the nanosilica particles are agglomerated in the dispersion, the agglomeration is mainly due to the interactions between

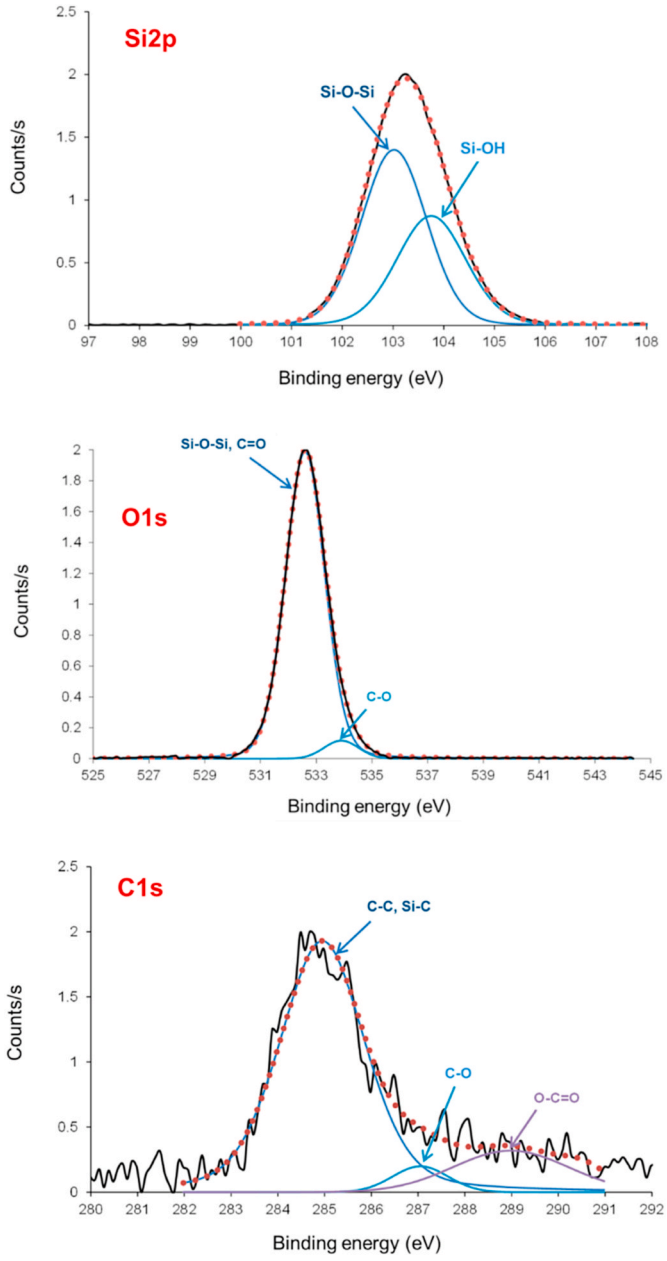

Fig. 5. High resolution XPS spectra of the nanosilica powder surface.

the acrylic moieties on the surface.

3.2. Characterization of the waterborne polyurethane dispersions

In order to produce an adequate dispersion of the nanosilica in the waterborne polyurethane dispersions, in this study different physical mixing procedures were used, they differ in the rheological flow regime and the stirring rate: (i) Anchor stirrer and low stirring rate (200 rpm) - PU + SiH; (ii) ViscoJet® stirrer and high stirring rate (1500 rpm) - PU + Si2H; and (iii) Double centrifuge SpeedMixer® and high stirring rate (2400 rpm) - PU + SiSM.

Some properties of the waterborne polyurethane dispersions (PUDs) with and without nanosilica are shown in Table 1. No sedimentation of the nanosilica particles in the PUDs was noticed over time. The solids contents of the dispersions are 48–50 wt% and, within the experimental error, they can be considered similar. On the other hand, the pH values of the PUDs without and with nanosilica are 7.9–8.0, because a small amount of nanosilica dispersion was added.

Table 1
Some properties of the waterborne polyurethane dispersions.

Dispersion	Solids content (wt. %)	pH	Z potential (mV)	Surface tension (mN/m)
PUD	49.7 ± 1.0	7.9 ± 0.0	−57	49.3 ± 0.0
PUD + SiH	48.8 ± 0.8	7.9 ± 0.1	−61	52.8 ± 0.5
PUD + SiSM	47.9 ± 0.2	7.9 ± 0.0	−68	58.6 ± 1.2
PUD + Si2H	49.2 ± 0.7	8.0 ± 0.0	−79	59.7 ± 0.0

The magnitude of the zeta (Z) potential indicates the degree of electrostatic repulsion between adjacent similarly charged particles in a dispersion. The Z potential values of the PUDs are negative because the waterborne polyurethane is anionic and the nanosilica particles in the aqueous dispersion are negatively charged. The Z potential of the PUDs becomes more negative by adding nanosilica because the lower Z potential value of the nanosilica dispersion (−87 mV) with respect to the one of the PUD without nanosilica (−57 mV); however, the Z potential varies with the physical mixing procedure, the more negative value corresponds to PUD + Si2H, this is an indication of a different degree of dispersion of the nanosilica in the waterborne polyurethane. Similarly, the surface tension values of the PUDs increase by adding nanosilica because the surface tension of the nanosilica dispersion (52.8 mN/m) is higher than the one of the PUD without nanosilica (49.3 mN/m), more markedly when higher stirring rates are used (PU + SiSM and PU + Si2H). Therefore, the physical mixing procedure determines the degree of nanosilica dispersion in the PUDs.

Fig. 6 shows the particle size distributions of the PUDs. The PUD without nanosilica is monomodal with a mean particle size of 217 nm and there are also 22% polyurethane particles of 250 nm and 11% polyurethane particles of 300 nm. The addition of nanosilica broads the particle size distribution of the PUD and decreases the mean particle size (from 217 nm to 194–206 nm), the lowest mean particle size corresponds to PUD + SiH. The increasing of the stirring rate during the physical mixing of the dispersions increases the percentage of particles higher than 300 nm from 11% to 20–29%, the higher percentage corresponds to the PUD + nanosilica dispersions made with high stirring rates, i.e., PUD + SiSM and PUD + Si2H. Therefore, a mild stirring facilitates the dispersion of the smallest nanosilica particles among the polyurethane particles. However, the highest stirring rate causes the partial rupture of the nanosilica clusters causing a broadening of the particle size distribution of the PUD due to the increase of the percentage of particles higher than 300 nm. Therefore, some nanosilica particles are well dispersed in the waterborne polyurethane dispersion but a significant number of them are agglomerated, in a different extent depending on the physical mixing procedure.

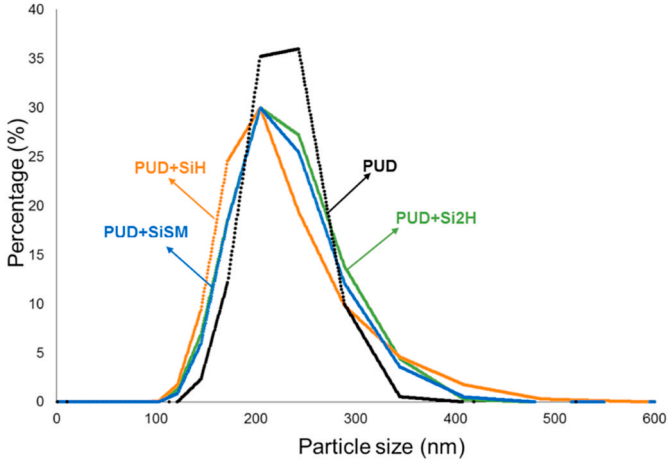

Fig. 6. Particle size distributions of the waterborne polyurethane dispersions.

Fig. 7 shows the variation of the Brookfield viscosity of the PUDs as a function of the shear rate. Because the Brookfield viscosity of the nanosilica dispersion (11 mPa s) is significantly lower than the one of the PUD, the addition of the nanosilica dispersion decreases the Brookfield viscosities of the PUDs from 140 mPa s in the PUD without nanosilica to 105–109 mPa s in the PUDs containing nanosilica (Table 2), i.e., the physical mixing procedure does not significantly affect the Brookfield viscosities of the PUDs. On the other hand, whereas the nanosilica dispersion shows a Newtonian rheological behavior, the PUDs show shear thinning, i. e, the viscosity decreases by increasing the shear rate. The extent of shear thinning was quantified by the ratio of the Brookfield viscosities at 1 and 20 s^{-1} (pseudoplastic index). The pseudoplastic index of the PUD decreases by adding nanosilica, the lowest value corresponds to PUD + Si2H (Table 2). The shear thinning in PUD is caused by the rupture of the interactions between the polyurethane particles. The less shear thinning in the PUDs containing nanosilica is caused by the intercalation of the nanosilica particles between the polyurethane particles reducing their interactions, more efficiently by increasing the stirring rate during the physical mixing of the dispersions.

In summary, the nanosilica particles intercalates between the polyurethane particles in the PUDs, the addition of nanosilica increases the surface tension and produces more negative Z potential values. Furthermore, the mean particle size, Brookfield viscosity, and the extent of shear thinning decrease. The physical mixing procedure determines differently the variation of those properties, the higher the stirring rate, the more pronounced change of the properties.

3.3. *Characterization of the nanosilica-waterborne polyurethanes*

Upon evaporation of the water in the PUDs, solid nanosilica-waterborne polyurethane (PU + nanosilica) materials were obtained, their structural properties were studied by ATR-IR spectroscopy, DSC and TGA, the degree of the dispersion of the nanosilica particles in the polyurethane matrix was analyzed by TEM, the viscoelastic properties were determined by plate-plate rheology, and the mechanical properties were assessed by stress-strain experiments.

The ATR-IR spectra of the PU + nanosilica materials (Figure A-1 of the Supplementary material file and Fig. 8) show the typical bands of the hard segments (N–H stretching at 3350-3400 cm^{-1}, C═O stretching of urethane at 1729 cm^{-1}, C–N and N–H bending at 1531 cm^{-1}, COO bending of urethane group at 736 cm^{-1}) and the soft segments (C–H stretching at 2950 and 2870 cm^{-1}, C–H bending at 1464 and 1370 cm^{-1}, C–H bending in CH_2CO group at 1420 cm^{-1}, and C–O–C stretching at 1238, 1170, 1140, 1068 and 960 cm^{-1}). The addition of nanosilica

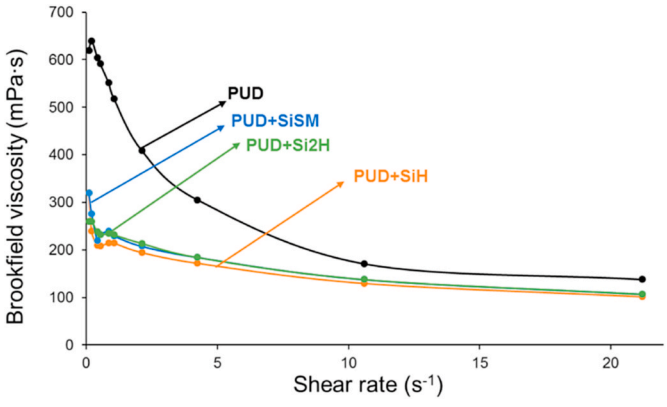

Fig. 7. Variation of Brookfield viscosity of the waterborne polyurethane dispersions as a function of the shear rate.

Table 2
Brookfield viscosities and pseudoplastic indexes of the waterborne polyurethane dispersions.

Dispersion	Viscosity at 20 s^{-1} (mPa s)	Pseudoplastic index
PUD	140	3.6
PUD + SiH	105	2.5
PUD + SiSM	109	2.3
PUD + Si2H	109	1.8

changes the intensities of the C–O–C stretching bands of the soft segments of the polyurethane at 1238, 1140 and 1068 cm^{-1}, more noticeably in PU + Si2H, these changes indicates the intercalation of the nanosilica particles between the soft segments [46]. As a consequence, the addition of nanosilica increases the intensity of the C–H stretching bands of the soft segments at 2950 and 2870 cm^{-1}. On the other hand, low intensity band at 1089 cm^{-1} due to the nanosilica can be distinguished. The intercalation of the nanosilica particles among the soft segments will cause a change of the physical interactions between the soft segments which can be evidenced better by DSC.

The structural changes in the PU + nanosilica materials were assessed by DSC. The DSC curves of the first heating run (Figure A-2a of the Supplementary material file and Fig. 9a) shows the glass transition of the soft segments at (−48 °C) – (−50 °C) and the melting of the soft segments. The melting of the soft segments in the PU without nanosilica shows two contributions at 32 °C and 51 °C, and the addition of nanosilica decreases the temperature and enthalpy of the melting contribution at 32 °C and increases the enthalpy of the melting contribution at 51 °C (Table 3a), this indicates the intercalation of the nanosilica particles between the polyurethane chains and the existence of two different structures of the soft segments, one without and another with intercalated nanosilica.

The DSC curves of the cooling run of the PU + nanosilica materials show the crystallization of the soft segments in the polyurethane (Fig. 9b). Whereas the crystallization peak appears at −7 °C in PU and PU + SiH with a crystallization enthalpy of 30–33 J/g, the peak displaces to higher temperature (0 °C) and shows higher crystallization enthalpy (40–41 J/g) in PU + SiSM and PU + Si2H, this confirm the intercalation of the nanosilica particles between the polyurethane chain in the PU + nanosilica materials obtained by physical mixing of the waterborne polyurethane and nanosilica dispersion by using high stirring rates.

After allowing a slow reorganization of the polyurethane chains, a second DSC heating run of the PU + nanosilica materials was carried out (Figure A-2b of the supplementary material file and Fig. 9c). The DSC curves of all PUs show the glass transitions of the soft (T_{g1}) and hard (T_{g2}) segments, and the melting of the soft segments. The DSC curves of PU and PU + SiH also show a cool crystallization at −21 °C which is absent in PU + SiSM and PU + Si2H because of the intercalation of the nanosilica particles between the soft segments of the polyurethane when the physical mixing is carried out with high stirring rates (Fig. 10). The addition of nanosilica by using high stirring rates increases the glass transition temperature of the soft segments (Table 3b) indicating lower degree of phase separation. However, the glass transition temperature of the hard segments is not affected by adding nanosilica (236–238 °C) because they do not interact with the nanosilica particles. On the other hand, the melting of the soft segments is complex and two contributions can be distinguished at 41–42 °C and 48–49 °C (Table 3b), the melting temperatures and enthalpies at 41–42 °C are higher than in the DSC curves of the first heating run (Table 3a) because more net interactions between the nanosilica and the soft segments. Therefore, two different structures of the soft segments can be distinguished in the PU +

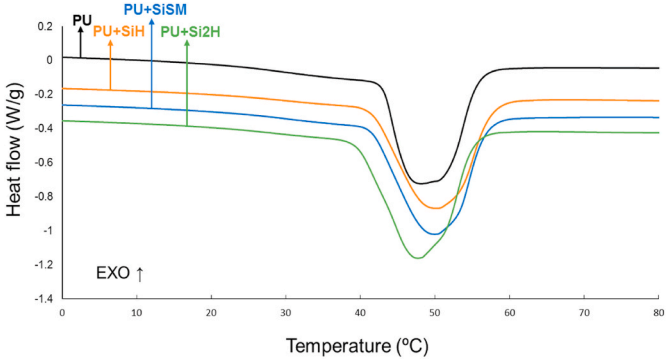

Fig. 9a. DSC curves of the PU + nanosilica materials. Melting region of the first heating run.

Table 3a
Some parameters obtained from the DSC curves of the PU + nanosilica materials. First heating run.

Material	T_g (°C)	T_{m1} (°C)	ΔH_{m1} (J/g)	T_{m2} (°C)	ΔH_{m2} (J/g)
PU	−49	32	7	51	40
PU + SiH	−49	31	4	53	43
PU + SiSM	−48	31	5	52	44
PU + Si2H	−50	29	5	51	44

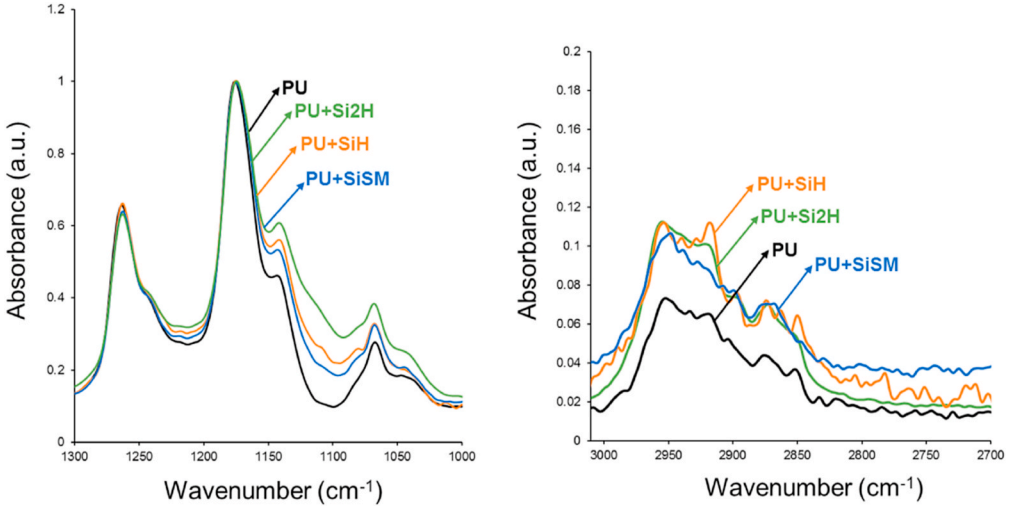

Fig. 8. Some regions of the ATR-IR spectra of the PU + nanosilica materials.

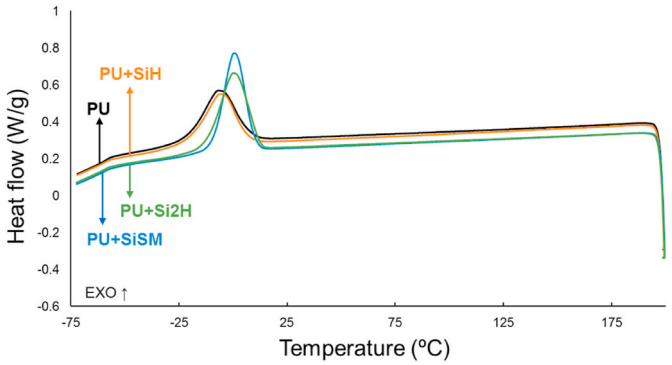

Fig. 9b. DSC curves of the PU + nanosilica materials. Cooling run.

nanosilica materials, one without and another with intercalated nanosilica. Furthermore, the melting temperatures are slightly higher in PU + SiSM and PU + Si2H than in the other PUs.

The structural changes in the PU + nanosilica materials were also assessed by TGA. The TGA curves of Fig. 11a show two main thermal decompositions at 260 °C and 350 °C due to the hard and soft domains respectively. The addition of nanosilica by physical mixing under high stirring rate increases the thermal stability of the polyurethanes due to the nanosilica-polyurethane interactions, in agreement with previous study [31]. In fact, the temperatures at which 5 ($T_{5\%}$) and 50 ($T_{50\%}$) mass loss are produced, are higher in PU + SiSM and PU + Si2H (Table 4). However, similar lower $T_{5\%}$ and $T_{50\%}$ values are obtained in PU and PU + SiH (Table 4).

The structural changes in the PU + nanosilica materials evidenced by TGA can be better distinguished in the derivative of the TGA curves (Fig. 11b). All PUs show five thermal decompositions at 51–55 °C (residual water), 230–255 °C (urethane and urea hard domains), 329–347 °C (soft domains), 389–397 °C and 434–447 °C (by-products formed during the TGA experiments [28]). The most important weight loss corresponds to the soft domains at 329–347 °C, and the temperatures and weight losses of PU and PU + SiH are somewhat similar because insufficient interactions of the nanosilica particles with the polyurethane chains in PU + SiH. However, the temperatures of decomposition of PU + SiSM and PU + Si2H are higher than in PU because of the intercalation of the nanosilica particles among the polyurethane chains. On the other hand, the weight losses of the soft domains are lower and the ones of the hard domains are higher in PU + SiSM and PU + Si2H than in PU, this support the intercalation of the nanosilica particles between the polyurethane chains and the change in the degree of phase separation in the polyurethane caused by addition of nanosilica by physical mixing at high stirring rates.

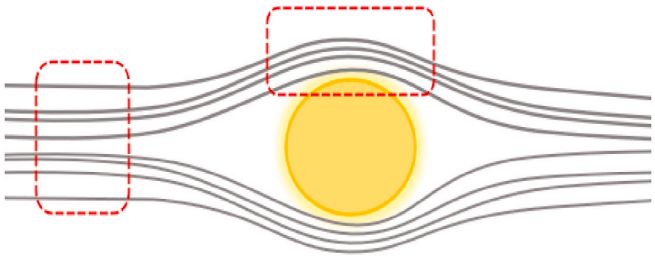

Fig. 10. Model of interactions between the polyurethane chains caused by intercalation of the nanosilica particles in which the two different interactions between the soft segments are cartooned (dotted red lines).

Table 3b
Some parameters obtained from the DSC curves of the PU + nanosilica materials. Second heating run.

Material	T_{g1} (°C)	T_{g2} (°C)	T_c (°C)	ΔH_c (J/g)	T_{m1} (°C)	ΔH_{m1} (J/g)	T_{m2} (°C)	ΔH_{m2} (J/g)
PU	−50	237	−21	2	41	11	48	29
PU + SiH	−51	236	−21	2	41	11	48	28
PU + SiSM	−48	236	–	–	42	13	49	28
PU + Si2H	−47	238	–	–	42	14	49	28

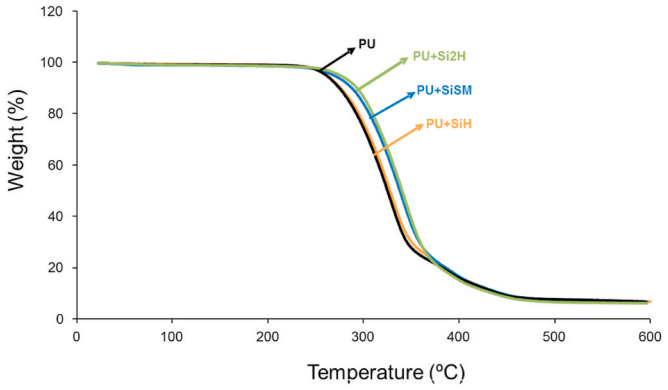

Fig. 11a. TGA curves of the PU + nanosilica materials.

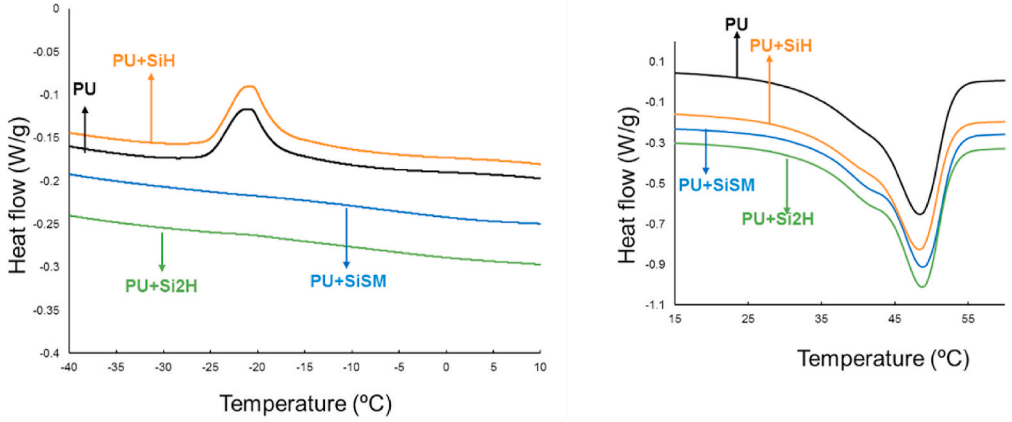

Fig. 9c. DSC curves of the PU + nanosilica materials. Cool crystallization (left) and melting (right) regions of the second heating run.

Table 4
Temperatures at which 5 ($T_{5\%}$) and 50 ($T_{50\%}$) % mass losses are produced in the PU + nanosilica materials. TGA experiments.

Material	$T_{5\%}$ (°C)	$T_{50\%}$ (°C)
PU	262	325
PU + SiH	262	328
PU + SiSM	269	337
PU + Si2H	276	340

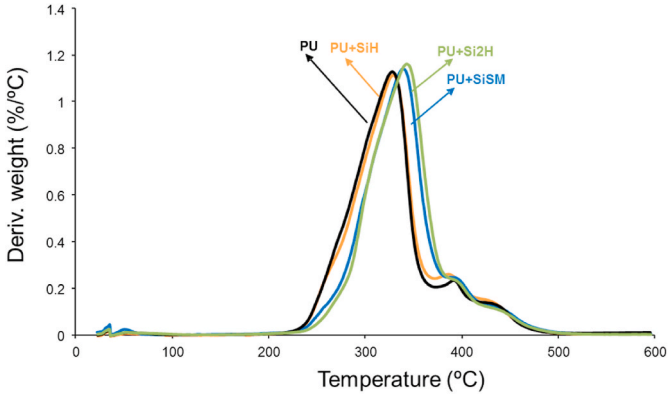

Fig. 11b. Derivative of TGA curves of the PU + nanosilica materials.

The extent of dispersion of the nanosilica particles in the polyurethane was assessed by TEM micrographs (Fig. 12). The TEM micrographs of the PU without nanosilica shows the phase separation of the hard (dark zones) and soft (light zones) domains [34], and the addition of nanosilica changes the degree of phase separation. The TEM micrographs of PU + SiH show the existence of agglomerates of nanosilica particles of about 120 nm length, but in minor zones some bundles of few nanosilica particles can be distinguished (Fig. 12). Therefore, the physical mixing at low stirring rate is not sufficient for breaking the nanosilica agglomerates in the dispersion and the structural changes in the polyurethane are minimal because insufficient intercalation of the most nanosilica particles, separated domains of nanosilica particles and polyurethane can be distinguished. However, the physical mixing of the waterborne polyurethane and the nanosilica dispersion using high stirring rates produces more effective dispersion of the nanosilica particles in the polyurethane matrix, more efficiently in PU + Si2H, because the TEM micrographs show several individual nanosilica particles and some small agglomerates of 15–35 nm length. On the other hand, the number of agglomerated nanosilica particles is somewhat lower in PU + Si2H than in PU + SiSM. Therefore, the efficient dispersion of the nanosilica particles in PU + Si2H and PU + SiSM agrees with the lower degree of phase separation in the polyurethane, the inhibition of the cold crystallization, and the increase of the thermal stability.

The structural changes in the PU + nanosilica materials should affect their viscoelastic properties, they were assessed by temperature sweep plate-plate rheological experiments. The variation of the storage (G') modulus of the PU + nanosilica materials as a function of the temperature shows a continuous decrease of G' by increasing the temperature (Fig. 13a), the rheological curves of PU and PU + SiH are similar. PU + SiSM shows the lowest G' values and, below the melting point of the PU + nanosilica materials, the G' values of PU+2Si2H are higher because of better dispersion of the nanosilica particles in the polyurethane matrix and lower number of nanosilica particles agglomerates.

All PU + nanosilica materials show a cross-over of the storage (G') and loss (G'') moduli (Fig. 13b). Above the cross-over temperature ($T_{cross\text{-}over}$) the materials are mainly elastic and below $T_{cross\text{-}over}$ they are mainly viscous. PU and PU + SiH have similar moduli at the cross-over ($5.2.10^{-2}$ MPa), but the $T_{cross\text{-}over}$ value is somewhat higher in PU + SiH because of the existence of abundant agglomerates of nanosilica

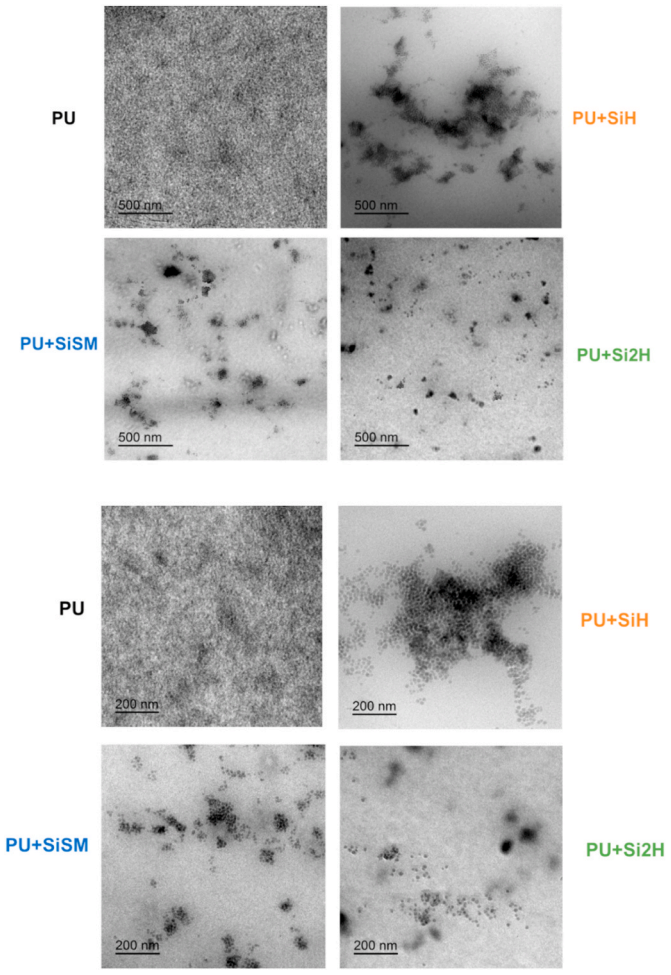

Fig. 12. TEM micrographs at different magnifications of the PU + nanosilica materials.

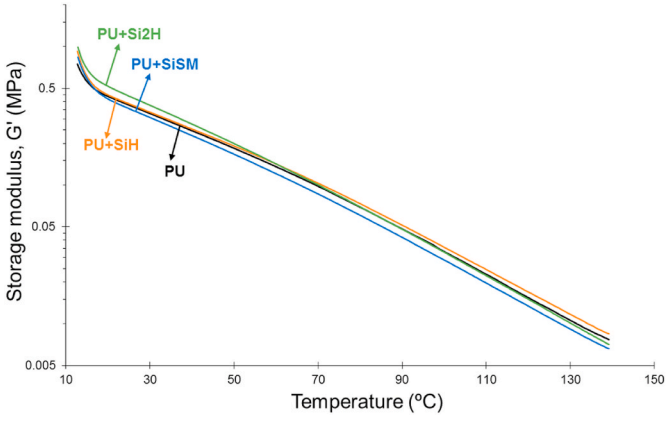

Fig. 13a. Variation of the storage modulus (G') as a function of the temperature for PU + nanosilica materials.

particles (Table 5). The $T_{cross\text{-}over}$ values of PU + SiSM and, more markedly, PU + Si2H are lower than the one of PU, and the modulus at the cross-over increases only in PU + Si2H because the lower percentage of nanosilica agglomerates (Table 5). Therefore, the viscoelastic properties of the PU + nanosilica materials are affected by the physical mixing procedure and stirring rate of the waterborne polyurethane and the nanosilica dispersion, and better viscoelastic properties are obtained when high stirring rates are used.

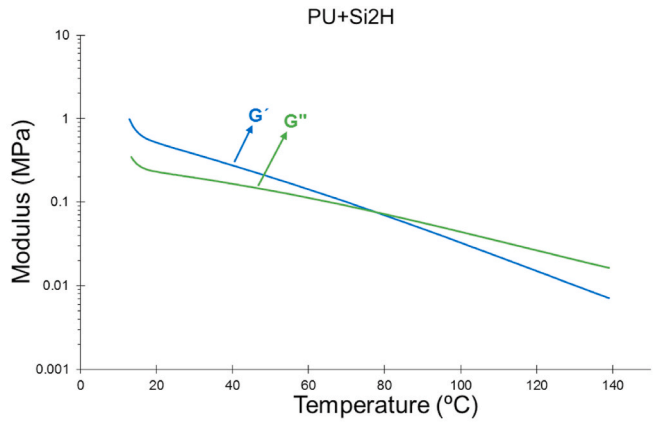

Fig. 13b. Variation of the storage (G') and loss (G'') moduli as a function of the temperature for PU + Si2H.

Table 5
Temperatures and moduli at the cross-over of the storage and loss moduli for PU + nanosilica materials. Plate-plate rheology experiments.

Material	$G_{cross\text{-}over}$ (MPa)	$T_{cross\text{-}over}$ (°C)
PU	$5.7 \bullet 10^{-2}$	84
PU + SiH	$5.6 \bullet 10^{-2}$	87
PU + SiSM	$5.6 \bullet 10^{-2}$	82
PU + Si2H	$7.6 \bullet 10^{-2}$	78

Previous studies are controversial with respect to the improvement of the mechanical properties of the waterborne polyurethanes by adding nanosilica. Whereas some literature [31,47] has shown improved mechanical properties of the PUDs by adding silicas, other literature evidenced the opposite trend [37] which was ascribed to the sedimentation of the silica particles. In this study, no sedimentation of the nanosilica particles was found, so improved mechanical properties can be expected in the PU + nanosilica materials.

The stress-strain curves of the PU + nanosilica materials show a marked yield point followed by an ample elastic deformation region (Fig. 14); at a strain of 500% (the highest reached in the equipment) none of the PU + nanosilica materials break, so the maximum strength was measured at a strain of 500%. PU + Si2H has somewhat better mechanical properties than PU, but they are inferior in PU + SiH and PU + SiSM (Fig. 14, Table 6). Whereas the addition of nanosilica does not change the value of the Young modulus (0.8–0.9 MPa), the yield stress values are lower in PU + SiH and PU + SiSM and the stress at 500% strain in PU + Si2H is the highest (Table 6). Therefore, the mechanical properties of the PU + nanosilica materials decrease in PU + SiH and PU + SiSM because of the existence of nanosilica agglomerates and increases moderately in PU + Si2H in which the most nanosilica particles are well dispersed in the polyurethane. Therefore, the trends in the mechanical properties found in this study are related to the percentages of nanosilica agglomerates in the PU + nanosilica materials.

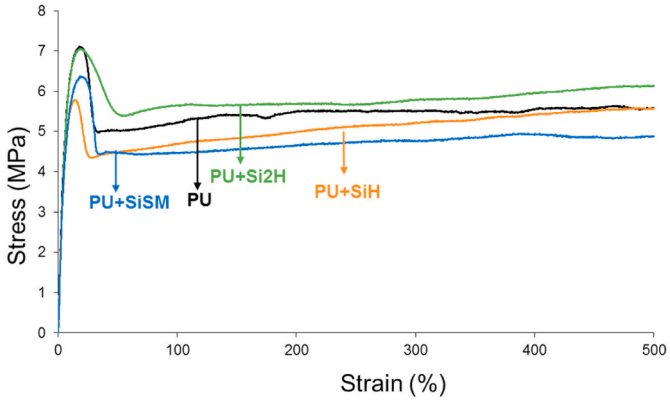

Fig. 14. Stress-strain plots of the PU + nanosilica materials.

Table 6
Some mechanical properties and water contact angle values of the PU + nanosilica materials. Stress-strain experiments.

Property	PU	PU + SiH	PU + SiSM	PU + Si2H
Young modulus (MPa)	0.9 ± 0.0	0.8 ± 0.0	0.8 ± 0.1	0.9 ± 0.1
Yield stress (MPa)	7.0 ± 0.2	5.9 ± 0.1	6.4 ± 0.2	7.0 ± 0.3
Stress at 500% (MPa)	5.5 ± 0.3	5.5 ± 0.4	4.9 ± 0.1	6.2 ± 0.1
Water contact angle (degrees)	68 ± 2	70 ± 1	71 ± 2	83 ± 1

In summary, the physical mixing procedure and the stirring rate during the mixing of the waterborne polyurethane and the nanosilica dispersions determine the extent of dis-agglomeration of the nanosilica particles and the dispersion of the nanosilica between the soft segments of the polyurethane. The physical mixing by using ViscoJet® stirrer at high shear rate (PU + Si2H material) is the most efficient for dispersing the nanosilica particles into the polyurethane matrix. Thus, PU + Si2H shows higher thermal stability, lower degree of phase separation between the hard and soft domains, the cold crystallization is inhibited, and the viscoelastic and mechanical properties are improved.

3.4. Adhesion properties

Due of the structural changes in the waterborne polyurethane caused by adding nanosilica, a modification of its adhesion properties can be expected.

Because the adhesion is determined by the adequate wettability of the adhesive, the water contact angles on the PU + nanosilica surfaces were measured. The water contact angle on the PU surface is 68° (Table 6) which seems adequate for producing reasonable wettability. The addition of nanosilica increases the water contact angle values, mainly for PU + Si2H. This increase agrees with the degree of dispersion of the nanosilica particles in the polyurethane matrix because the surface tension of the nanosilica dispersion (63 mN/m) is significantly higher than the one of the waterborne polyurethane (49 mN/m). Because the wettability of the PU + Si2H surface is worse than the one of PU, the acrylic moieties of the nanosilica dispersion seem to migrate to the surface. As a consequence, the adhesion of the waterborne polyurethanes is not expected to increase when the nanosilica dispersion is added.

The influence of the addition of nanosilica dispersion to waterborne polyurethane on its adhesion properties is not clear in the existing literature. Both increased adhesion to different substrates [2,6,32,36] and lower adhesion [15] of silica-waterborne polyurethanes have been shown, the increased adhesion was related to the existence of interactions between the nanosilica and the polyurethane, and to the extent of nanosilica agglomeration.

The adhesion properties of the waterborne polyurethane dispersions without and with nanosilica were assessed by single lap-shear tests of stainless steel/PUD/stainless steel and by T-peel tests of plasticized PVC/PUD/plasticized PVC joints.

Table 7 shows the single lap-shear strength values of the stainless steel/PUD/stainless steel joints. The addition of nanosilica does not change the single lap-shear strength values, and decreases in the joint made with PUD + SiH. All joints show similar loci of failure, i.e. a cohesive failure of the adhesive (Fig. 15), so the cohesion of the PU + nanosilica materials is the weakest part of the joints. Because no sedimentation of nanosilica was found in the PUDs containing nanosilica,

Table 7
Single lap-shear strength values of stainless steel/polyurethane dispersion/stainless steel joints.

Dispersion	Lap-shear strength-72 h (kPa)	Locus of failure 72-h
PUD	776 ± 4	CA
PUD + SiH	630 ± 7	CA
PUD + SiSM	783 ± 11	CA
PUD + Si2H	751 ± 37	CA

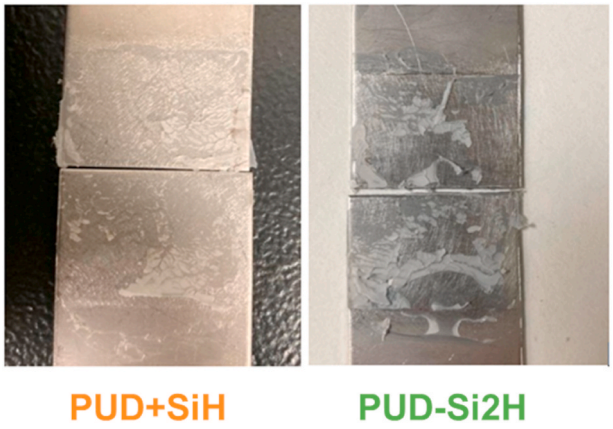

Fig. 15. Loci of failure of stainless steel/PUD/stainless steel joints.

the lack of improvement or the decrease in adhesion in the stainless steel/PUD/stainless steel joints made with PUD + SiSM or PUD + SiH can be ascribed to the existence of noticeable amounts of nanosilica agglomerates. However, the similar adhesion in the joints made with PUD and PUD + Si2H cannot be ascribed to the agglomeration of the nanosilica particles because the most of the nanoparticles are well dispersed in the polyurethane in PUD + Si2H.

The T-peel strength of plasticized PVC/PUD/plasticized PVC joints was monitored after 15 min (immediate adhesion) and 72 h (final adhesion) of joint formation (Table 8). A short time (15 min) after joint formation is not sufficient for complete removal of water in the PUDs and they are not completely cross-linked, so the T-peel strength values are somewhat low (2.0–3.7 kN/m) and the loci of failure in all joints is cohesive failure of the adhesive (Fig. 16 a)). The physical mixing procedure of the waterborne polyurethane and the nanosilica dispersion determines the immediate T-peel strength because the joint made with PUD + SiH shows a significant increase in the immediate adhesion even the existence of a high percentage of agglomerated nanosilica particles. On the contrary, the lowest immediate T-peel strength corresponds to the joint made with PUD + Si2H in which the most of the nanosilica particles are well-dispersed in the waterborne polyurethane. This unexpected trend in the immediate T-peel strength can be ascribed to the worse wettability of the PUD + nanosilicas made by using high stirring rates and to the absence of acrylic moieties from the functionalized nanosilica particles at the interface. It should be keep in mind that, 15 min after joint formation, the waterborne polyurethane dispersions are not completely cross-linked, so the migration of antiadherent moieties to the interface is not favoured.

Table 8
T-peel strength values of plasticized PVC/polyurethane dispersion/plasticized PVC joints at different times after joints formation.

Dispersion	T peel strength-15 min (kN/m)	Locus of failure-15 min	T peel strength-72 h (kN/m)	Locus of failure-72 h
PUD	2.3 ± 0.2	CA	15.3 ± 1.0	S
PUD + SiH	3.7 ± 0.3	CA	8.1 ± 0.5	S + SS
PUD + SiSM	2.5 ± 0.6	CA	7.7 ± 1.2	SS
PUD + Si2H	2.0 ± 0.8	CA	5.9 ± 0.9	SS

When the water in the PUD is completely removed (72 h), the T-peel strength of the plasticized PVC/PUD/plasticized PVC joints (final adhesion) increases with respect to the T-peel strength values obtained 15 min after joint formation (Table 8). The final T-peel strength values of the joints made with PUD + nanosilica dispersions are significantly lower than the one obtained with the PUD without nanosilica, the final adhesion is affected differently depending on the physical mixing procedure. The better the nanosilica dispersion in the PU + nanosilica, the lower the final T-peel strength value. Whereas the locus of failure of the joints made with the PUD without nanosilica is cohesive failure of the PVC (Fig. 16 b)), the one in the joints made with PUD + SiH is mixed (cohesive failure of the PVC + Cohesion in a surface layer of PVC) (Fig. 16 c)), and the one in the joints made with PUD + SiSM and PUD + Si2H is cohesion in a surface layer of PVC (Fig. 16 d). These experimental results agree with the lower wettability of PUD + Si2H and confirm the migration of acrylic moieties of the nanosilica particles to the surface, both contribute to decreased adhesion. In fact, the more dispersed nanosilica particles, the higher concentration of acrylic moieties on the adhesive surface. The deleterious adhesion of the waterborne polyurethane dispersions containing nanosilica has been previously ascribed to the migration of surfactant/antiadherent moieties to the interface, a change of the loci of failure from cohesive rupture to surface cohesive failure of the substrate was evidenced [48]. Similarly, it has been shown [14] that the adhesion of the waterborne polyurethane dispersions containing 1–5 wt% nanosilica made by physical mixing was lower than the one of the dispersion without nanosilica.

4. Conclusions

Waterborne polyurethane dispersions containing nanosilica have been successfully prepared by using different physical mixing procedures differing in the rheological flow regime and the stirring rate. The PUD + nanosilica dispersions were stable and showed no sedimentation over time.

The nanosilica dispersion showed a Newtonian rheological behavior, the surface tension was somewhat high (63 mN/m) and the most nanosilica particles were clustered forming agglomerates of about 150 nm. The nanosilica was functionalized with acrylic moieties which may be responsible of the agglomeration of the particles.

The Z potential became more negative and the surface tension of the PUDs increased by adding nanosilica, and they varied with the physical mixing procedure because of a different degree of dispersion of the nanosilica in the polyurethane. The more negative Z-potential and surface tension values corresponded to PUD + Si2H made at high stirring rate and under dynamic radial flow. The addition of nanosilica caused a broadening of the particle size distributions of the PUDs and reduced the mean particle size, the lowest mean particle size corresponded to PUD + SiH. On the other hand, the addition of nanosilica decreased the Brookfield viscosities of the PUDs, the physical mixing procedure did not affect the Brookfield viscosity. All PUDs showed shear thinning, the addition of nanosilica reduced the extent of shear thinning, more markedly when the physical mixing was carried out at high stirring rate, because the intercalation of the nanosilica particles between the polyurethane particles reduced their interactions.

Due to the intercalation of the nanosilica particles between the soft segments, the addition of nanosilica changed the intensities of the C–O–C stretching and increased the ones of the C–H stretching bands, more noticeably in PU + Si2H. As a consequence, the crystallization peak of the polyurethane displaced to higher temperature and increased crystallization enthalpies were obtained in PU + SiSM and PU + Si2H, and the cool crystallization disappeared. The addition of nanosilica at high stirring rates decreased the degree of phase separation in the polyurethane and increased the thermal stability due to the nanosilica-

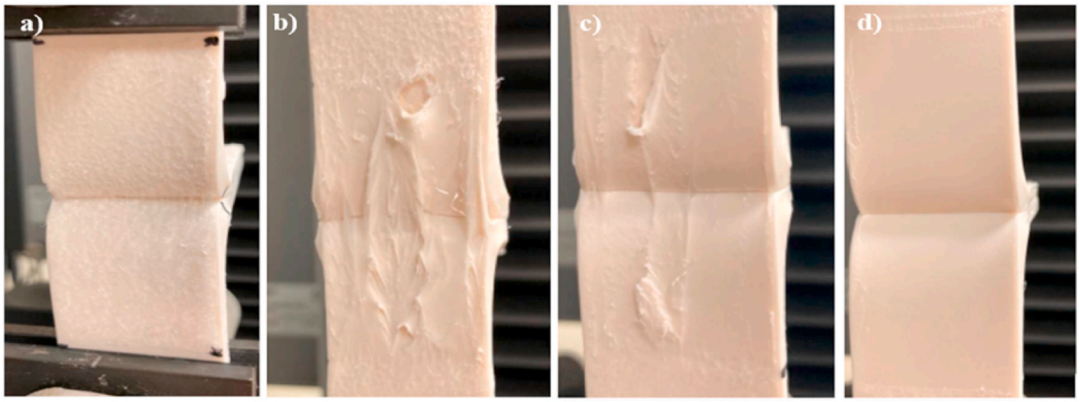

Fig. 16. Loci of failure of plasticized PVC/polyurethane dispersion/plasticized PVC joints. a) Cohesive failure of adhesive (CA); b) Substrate cohesive failure (S); c) Substrate cohesive failure (S) + Cohesion in a surface layer of the substrate (SS); d) Cohesion in a surface layer of the substrate (SS).

polyurethane interactions. The physical mixing of the dispersions at high stirring rates produced more efficient dispersion of the nanosilica particles in the polyurethane matrix, particularly in PU + Si2H in which several individual nanosilica particles and some small agglomerates of 15–35 nm length were distinguished. The viscoelastic and mechanical properties of the PU + nanosilica materials were affected by the physical mixing procedure and the stirring rate, and better properties were obtained in PU + Si2H because the less nanosilica agglomeration in the polyurethane.

Unexpectedly, the addition of nanosilica increased the water contact angle values of the PU + nanosilica materials, mainly for PU + Si2H, even better nanosilica dispersion was obtained, this was ascribed to the migration of acrylic moieties from the nanosilica particles to the surface.

The addition of nanosilica does not change or decrease the single lap-shear strength values. On the other hand, the physical mixing procedure of the dispersions determined the immediate T-peel strength and the joint made with PUD + SiH showed a significant increase even the existence of a high percentage of agglomerated nanosilica particles. On the contrary, the lowest immediate T-peel strength corresponded to the joint made with PUD + Si2H in which the most of the nanosilica particles are well-dispersed in the polyurethane. This unexpected trend in the immediate T-peel strength was ascribed to the worse wettability of the PUD + nanosilicas made at high stirring rates. Finally, the final T-peel strength values of the joints made with PUD + nanosilica dispersions were significantly lower than the one obtained with the PUD without nanosilica, the physical mixing procedure affected differently the final T-peel strength values. The better the nanosilica dispersion in the PU + nanosilica material, the lower the final T-peel strength value. These experimental results were explained by the lower wettability of PUD + Si2H and the migration of acrylic moieties of the nanosilica particles to the surface.

Declaration of competing interest

The authors declare that they have no known competing financial interests or personal relationships that could have appeared to influence the work reported in this paper.

Data availability

Data will be made available on request.

Acknowledgment

This study was partially supported by the Research Vice-president Office (Vicerrectorado de Investigación) of the University of Alicante (grant no. AII21-07).

Appendix A. Supplementary data

Supplementary data to this article can be found online at https://doi.org/10.1016/j.ijadhadh.2023.103342.

References

[1] Akindoyo JO, Beg MD, Ghazali S, Islam MR, Jeyaratnam N, Yuvaraj AR. Polyurethane types, synthesis and applications–A review. RSC Adv 2016;6(115):114453–82. https://doi.org/10.1039/C6RA14525F.
[2] Jia-Hu G, Yu-Cun L, Tao C, Su-Ming J, Hui M, Ning Q, Wei-Ming H. Synthesis and properties of a nano-silica modified environmentally friendly polyurethane adhesive. RSC Adv 2015;5(56):44990–7. https://doi.org/10.1039/C5RA01965F.
[3] Melchiors M, Sonntag M, Kobusch C, Jürgens E. Recent developments in aqueous two-component polyurethane (2K-PUR) coatings. Prog Org Coating 2000;40(1–4):99–109. https://doi.org/10.1016/S0300-9440(00)00123-5.
[4] Li R, Shan Z. Research for waterborne polyurethane/composites with heat transfer performance: a review. Polym Bull 2018;75(10):4823–36. https://doi.org/10.1007/s00289-018-2276-3.
[5] Tounici A, Martín-Martínez JM. Addition of small amounts of graphene oxide in the polyol during the synthesis of waterborne polyurethane urea adhesives for improving their adhesion properties. Int J Adhesion Adhes 2021;104:102725. https://doi.org/10.1016/j.ijadhadh.2020.102725.
[6] Maciá-Agulló TG, Fernández-García JC, Torró-Palau A, Orgilés Barceló AC, Martín-Martínez JM. Hydrophobic or hydrophilic fumed silica as filler of polyurethane adhesives. J Adhes 1995;50(4):265–77. https://doi.org/10.1080/00218469508014557.
[7] Mallakpour S, Naghdi M. Polymer/SiO_2 nanocomposites: production and applications. Prog Mater Sci 2018;97:409–47. https://doi.org/10.1016/j.pmatsci.2018.04.002.
[8] Lee SI, Hahn Bs Y, Nahm KS, Lee YS. Synthesis of polyether-based polyurethane-silica nanocomposites with high elongation property. Polym Adv Technol 2005;16(4):328–31. https://doi.org/10.1002/pat.548.
[9] Jeon HT, Jang MK, Kim BK, Kim KH. Synthesis and characterizations of waterborne polyurethane–silica hybrids using sol–gel process. Physicochem Eng Asp 2007;302(1–3):559–67. https://doi.org/10.1016/j.colsurfa.2007.03.043.
[10] Xia Y, Larock RC. Preparation and properties of aqueous castor oil-based polyurethane–silica nanocomposite dispersions through a sol–gel process. Macromol Rapid Commun 2011;32(17):1331–7. https://doi.org/10.1002/marc.201100203.
[11] Wu D, Qiu F, Xu H, Zhang J, Yang D. Preparation, characterization, and properties of environmentally friendly waterborne poly (urethane acrylate)/silica hybrids. J Appl Polym Sci 2011;119(3):1683–95. https://doi.org/10.1002/app.32846.
[12] Lai X, Shen Y, Wang L, Li Z. Preparation and performance of waterborne polyurethane/nanosilica hybrid materials. Polym-Plast Technol Eng 2011;50(7):740–7. https://doi.org/10.1080/03602559.2010.551442.
[13] Sardon H, Irusta L, Aguirresarobe RH, Fernández-Berridi M. Polymer/silica nanohybrids by means of tetraethoxysilane sol–gel condensation onto waterborne polyurethane particles. Prog Org Coating 2014;77(9):1436–42. https://doi.org/10.1016/j.porgcoat.2014.04.032.
[14] Heck CA, dos Santos JHZ, Wolf CR. Waterborne polyurethane: the effect of the addition or in situ formation of silica on mechanical properties and adhesion. Int J Adhesion Adhes 2015;58:13–20. https://doi.org/10.1016/j.ijadhadh.2014.12.006.
[15] Cakić SM, Valcic MD, Ristic IS, Radusin T, Cvetinov MJ, Budinski-Simendić J. Waterborne polyurethane-silica nanocomposite adhesives based on castor oil-recycled polyols: effects of (3-aminopropyl) triethoxysilane (APTES) content on properties. Int J Adhesion Adhes 2019;90:22–31. https://doi.org/10.1016/j.ijadhadh.2019.01.005.

[16] Meng L, Zhu H, Feng B, Gao Z, Wang D, Wei S. Embedded polyhedral SiO_2/castor oil-based WPU shell-core hybrid coating via self-assembly sol-gel process. Prog Org Coating 2020;141:105540. https://doi.org/10.1016/j.porgcoat.2020.105540.
[17] Wang H, Wang H, Xu J, Du X, Yang S, Wang H. Thermo-driven self-healable organic/inorganic nanohybrid polyurethane film with excellent mechanical properties. Polym J 2022;54(3):293–303. https://doi.org/10.1038/s41428-021-00563-2.
[18] Chen JJ, Zhu CF, Deng HT, Qin ZN, Bai YQ. Preparation and characterization of the waterborne polyurethane modified with nanosilica. J Polym Res 2009;16(4):375–80. https://doi.org/10.1007/s10965-008-9238-7.
[19] Cheng L, Zhang X, Dai J, Liu S. Characterization of the waterborne polyurethane/nanosilica composite synthesized by dispersing nanosilica in polytetrahydrofuran glycol. J Dispersion Sci Technol 2012;33(6):840–5. https://doi.org/10.1080/01932691.2011.579859.
[20] Gao X, Zhu Y, Zhao X, Wang Z, An D, Ma Y, Guan S, Du Y, Zhou B. Synthesis and characterization of polyurethane/SiO_2 nanocomposites. Appl Surf Sci 2011;257(10):4719–24. https://doi.org/10.1016/j.apsusc.2010.12.138.
[21] Han Y, Chen Z, Dong W, Xin Z. Improved water resistance, thermal stability, and mechanical properties of waterborne polyurethane nanohybrids reinforced by fumed silica via in situ polymerization. High Perform Polym 2015;27(7):824–32. https://doi.org/10.1177/0954008314563058.
[22] Yan-ting H, Zheng C, Wei D, Fan Z, Zhong-yin X. Comparative study of in situ polymerized waterborne polyurethane/nano-silica composites and polyethersiloxanediol-modified polyurethane. J Thermoplast Compos Mater 2017;30(1):107–20. https://doi.org/10.1177/0892705715584434.
[23] Han Y, Hu J, Xin Z. In-situ incorporation of alkyl-grafted silica into waterborne polyurethane with high solid content for enhanced physical properties of coatings. Polymers 2018;10(5):514. https://doi.org/10.3390/polym10050514.
[24] Sardon H, Irusta L, Fernández-Berridi MJ, Lansalot M, Bourgeat-Lami E. Synthesis of room temperature self-curable waterborne hybrid polyurethanes functionalized with (3-aminopropyl) triethoxysilane (APTES). Polymer 2010;51(22):5051–7. https://doi.org/10.1016/j.polymer.2010.08.035.
[25] Xiaojuan L, Xiaorui L, Lei W, Yiding S. Synthesis and characterizations of waterborne polyurethane modified with 3-aminopropyltriethoxysilane. Polym Bull 2010;65(1):45–57. https://doi.org/10.1007/s00289-009-0233-x.
[26] Zhou Wang HH, Tian X, Zheng K, Cheng Q. Effect of 3-aminopropyltriethoxysilane on polycarbonate based waterborne polyurethane transparent coatings. Prog Org Coating 2014;77(6):1073–8. https://doi.org/10.1016/j.porgcoat.2014.03.006.
[27] Wang G, Ma G, Hou C, Guan T, Ling L, Wang B. Preparation and properties of waterborne polyurethane/nanosilica composites: a diol as extender with triethoxysilane group. J Appl Polym Sci 2014;131(15). https://doi.org/10.1002/app.40526.
[28] Gurunathan T, Chung JS. Physicochemical properties of amino–silane-terminated vegetable oil-based waterborne polyurethane nanocomposites. ACS Sustainable Chem Eng 2016;4(9):4645–53. https://doi.org/10.1021/acssuschemeng.6b00768.
[29] Sun D, Miao X, Zhang K, Kim H, Yuan Y. Triazole-forming waterborne polyurethane composites fabricated with silane coupling agent functionalized nano-silica. J Colloid Interface Sci 2011;361(2):483–90. https://doi.org/10.1016/j.jcis.2011.05.062.
[30] Ding X, Wang X, Zhang H, Liu T, Hong C, Ren Q, Zhou C. Preparation of waterborne polyurethane-silica nanocomposites by a click chemistry method. Mater Today Commun 2020;23:100911. https://doi.org/10.1016/j.mtcomm.2020.100911.
[31] Yang CH, Liu J F, Liu YP, Liao WT. Hybrids of colloidal silica and waterborne polyurethane. J Colloid Interface Sci 2006;302(1):123–32. https://doi.org/10.1016/j.jcis.2006.06.001.
[32] Cakić SM, Ristić IS, Milena M, Stojiljković DT, Jaroslava B. Preparation and characterization of waterborne polyurethane/silica hybrid dispersions from castor oil polyols obtained by glycolysis poly (ethylene terephthalate) waste. Int J Adhesion Adhes 2016;70:329–41. https://doi.org/10.1016/j.ijadhadh.2016.07.010.
[33] Serkis M, Špírková M, Hodan J, Kredatusová J. Nanocomposites made from thermoplastic waterborne polyurethane and colloidal silica. The influence of nanosilica type and amount on the functional properties. Prog Org Coating 2016;101:342–9. https://doi.org/10.1016/j.porgcoat.2016.07.021.
[34] Peruzzo PJ, Anbinder PS, Pardini FM, Pardini OR, Plivelic TS, Amalvy JI. On the strategies for incorporating nanosilica aqueous dispersion in the synthesis of waterborne polyurethane/silica nanocomposites: effects on morphology and properties. Mater Today Commun 2016;6:81–91. https://doi.org/10.1016/j.mtcomm.2016.01.002.
[35] Heck CA, dos Santos JHZ, Wolf CR. Hybrid silicas/waterborne polyurethane composite properties: in situ formation vs. grafting methods. J Sol Gel Sci Technol 2017;81(2):505–13. https://doi.org/10.1007/s10971-016-4220-z.
[36] Špírková M, Pavličević J, Aguilar Costumbre Y, Hodan J, Krejčíková S, Brožová L. Novel waterborne poly (urethane-urea)/silica nanocomposites. Composites 2020;41(10):4031–42. https://doi.org/10.1002/pc.25690.
[37] Boonsong K, Khaokong C. Preparation of anionic waterborne polyurethane composites with silica from rice husk ash. J Polym Res 2022;29(2):1–17. https://doi.org/10.1007/s10965-022-02903-z.
[38] Sanchez F, Sobolev K. Nanotechnology in concrete–A review. Construct Build Mater 2010;24(11):2060–71. https://doi.org/10.1016/j.conbuildmat.2010.03.014.
[39] Feng LB, Wang YP, Qiang XH, Wang SH. Effect of silica nanoparticles on properties of waterborne polyurethanes. Chin J Polym Sci 2012;30(6):845–52.
[40] Chiacchiarelli LM, Puri I, Puglia D, Kenny JM, Torre L. The relationship between nanosilica dispersion degree and the tensile properties of polyurethane nanocomposites. Colloid Polym Sci 2013;291(12):2745–53. https://doi.org/10.1007/s00396-013-3019-5.
[41] Muhamad MS, Salim MR, Lau WJ. Surface modification of SiO_2 nanoparticles and its impact on the properties of PES-based hollow fiber membrane. RSC Adv 2015;5(72):58644–54. https://doi.org/10.1039/C5RA07527K.
[42] Bywalez R, Karacuban H, Nienhaus H, Schulz C, Wiggers H. Stabilization of mid-sized silicon nanoparticles by functionalization with acrylic acid. Nanoscale Res Lett 2012;7:76. https://doi.org/10.1186/1556-276X-7-76.
[43] Feng L, Yang H, Dong X, Lei H, Chen D. pH-sensitive polymeric particles as smart carriers for rebar inhibitors delivery in alkaline condition. J Appl Polym Sci 2018:45886. https://doi.org/10.1002/APP.45886.
[44] Post P, Wurlitzer L, Maus-Friedrichs W, Weber AP. Characterization and applications of nanoparticles modified in-flight with silica or silica-organic coatings. Nanomaterials 2018;8:530. https://doi.org/10.3390/nano8070530.
[45] Hashemi A, Bahari A. Structural and dielectric characteristic of povidone–silica nanocomposite films on the Si (n) substrate. Appl Phys A 2017;123:535. https://doi.org/10.1007/s00339-017-1152-6.
[46] Lin WC, Yang CH, Wang TL, Shieh YT, Chen WJ. Hybrid thin films derived from UV-curable acrylate-modified waterborne polyurethane and monodispersed colloidal silica. Express Polym Lett 2012;6(1):2–13. https://doi.org/10.3144/expresspolymlett.2012.2.
[47] Santamaria-Echart A, Fernandes I, Barreiro F, Corcuera MA, Eceiza A. Advances in waterborne polyurethane and polyurethane-urea dispersions and their eco-friendly derivatives: a review. Polymers 2021;13(3):409. https://doi.org/10.3390/polym13030409.
[48] Anandhan S, Lee Sh H. Influence of organically modified clay mineral on domain structure and properties of segmented thermoplastic polyurethane elastomer. J Elastomers Plastics 2014;46(3):217–32. https://doi.org/10.1177/0095244312465300.